Astron. Astrophys. 354, 1036–1040 (2000)

ASTRONOMY AND ASTROPHYSICS

Probing the properties of methyl cyanide sources

S.V. Kalenskii[1], **V.G. Promislov**[1], **A.V. Alakoz**[1,3] **A. Winnberg**[2], **and L.E.B. Johansson**[2]

[1] Astro Space Center of Lebedev Physical Institute, Profsoyuznaya 84/32, 117810 Moscow, Russia (kalensky@dpc.asc.rssi.ru; vitaly@diogen.asc.rssi.ru; alakoz@dpc.asc.rssi.ru)
[2] Onsala Space Observatory, 439 92 Onsala, Sweden (anders@oso.chalmers.se; leb@oso.chalmers.se)
[3] Moscow State University, Physical Faculty, Astronomical Department, Universitetskii pr. 13, 119899 Moscow, Russia

Received 18 September 1998/ Accepted 22 December 1999

Abstract. A survey of 27 galactic star-forming regions in the $6_K - 5_K$ and $5_K - 4_K$ CH_3CN lines at 110 and 92 GHz, respectively, was made. Twenty-five sources were detected at 110 GHz and nineteen at 92 GHz. The strongest CH_3CN emission arise in hot cores in the regions of massive star formation. CH_3CN abundance in these objects is increased up to 10^{-9} or larger. Weaker CH_3CN lines were found in a number of sources. They may arise in warm (30–50 K) clouds.

Key words: ISM: clouds – ISM: molecules – ISM: abundances – radio lines: ISM

1. Introduction

Methyl cyanide (CH_3CN) is a symmetric top molecule. Like other molecules of this type, e.g., ammonia or methyl acetylene, methyl cyanide is a good temperature probe for interstellar gas. To date only a few CH_3CN surveys have been published, each of them devoted to a relatively small number of objects (Bergman & Hjalmarson 1989; Churchwell et al. 1992; Olmi et al. 1993). Therefore we made a more extended survey of Galactic star-forming regions in the $6_K - 5_K$ and $5_K - 4_K$ series of methyl cyanide lines near 110 and 92 GHz, respectively, to search for new CH_3CN sources and determine their temperatures and some other properties.

2. Observations

The observations were carried out in April–May 1996 using the 20-m millimetre-wave telescope of Onsala Space Observatory. The pointing accuracy was checked by the observatons of strong SiO masers; in all cases the errors were found to be less than $5''$. Main beam efficiency and half-power beamwidth at 92 GHz were 0.55 and $39''$, respectively. The observations were performed in a dual-beam switching mode with a switch frequency of 2 Hz and a beam separation of $11'$. The system noise temperature varied at both frequencies between 350 and 2000 K. The data were calibrated using the standard chopper-wheel method. The backend consisted of two parallel filter spectrometers: a 256-channel spectrometer with 250 kHz frequency resolution and a 512-channel spectrometer with 1 MHz frequency resolution. NGC 1333 IRAS2 and L 1157 were observed only with the 1 MHz resolution.

At 110 GHz 27 sources were observed. Of those 19 were observed at 92 GHz. The Gaussian parameters of the lines were obtained assuming that different K-components within each series have common LSR velocities and linewidths.

Send offprint requests to: A. Winnberg

3. Results

Emission at 110 GHz was detected towards 25 objects (S 252, W 48 and DR 21 West were only marginally detected). At 92 GHz, emission was found toward 16 objects. The spectra at 110 and 92 GHz are presented in Figs. 1 and 2, respectively. The source coordinates and the gaussian parameters of the detected lines are given in Table 1.

A weak blend of the $5_0 - 4_0$ and $5_1 - 4_1$ $CH_3^{13}CN$ lines at 91941.596 and 91939.834 MHz, respectively, was found towards G34.26+0.15. The ratios of the $CH_3^{13}CN/CH_3^{12}CN$ line intensities are about 0.15, i.e., much higher than the expected abundance of ^{13}C relative to ^{12}C, strongly suggesting that the CH_3CN lines are optically thick. This assumption was confirmed by statistical equilibrium (SE) calculations (see below). Similar ratios between the $6_K - 5_K$ $CH_3^{13}CN/CH_3^{12}CN$ line intensities in G34.26+0.15 were found by Akeson & Carlstrom (1996).

4. Statistical equilibrium calculations

To determine the source properties by means of statistical equilibrium (SE) calculations, we used a similar approach as e.g., Bergman & Hjalmarson (1989) and Olmi et al. (1993). This approach suggests that the sources are homogeneous and the LVG technique is applicable. We performed LVG calculations for a number of parameter sets and choose the sets which are in agreement with the observational data. The agreement between our observations and SE models can be evaluated by comparing model ratios of line brightness temperatures within the 110 and 92 GHz series with the corresponding observed ratios of main-beam brightness temperatures. For the 110 GHz lines we used

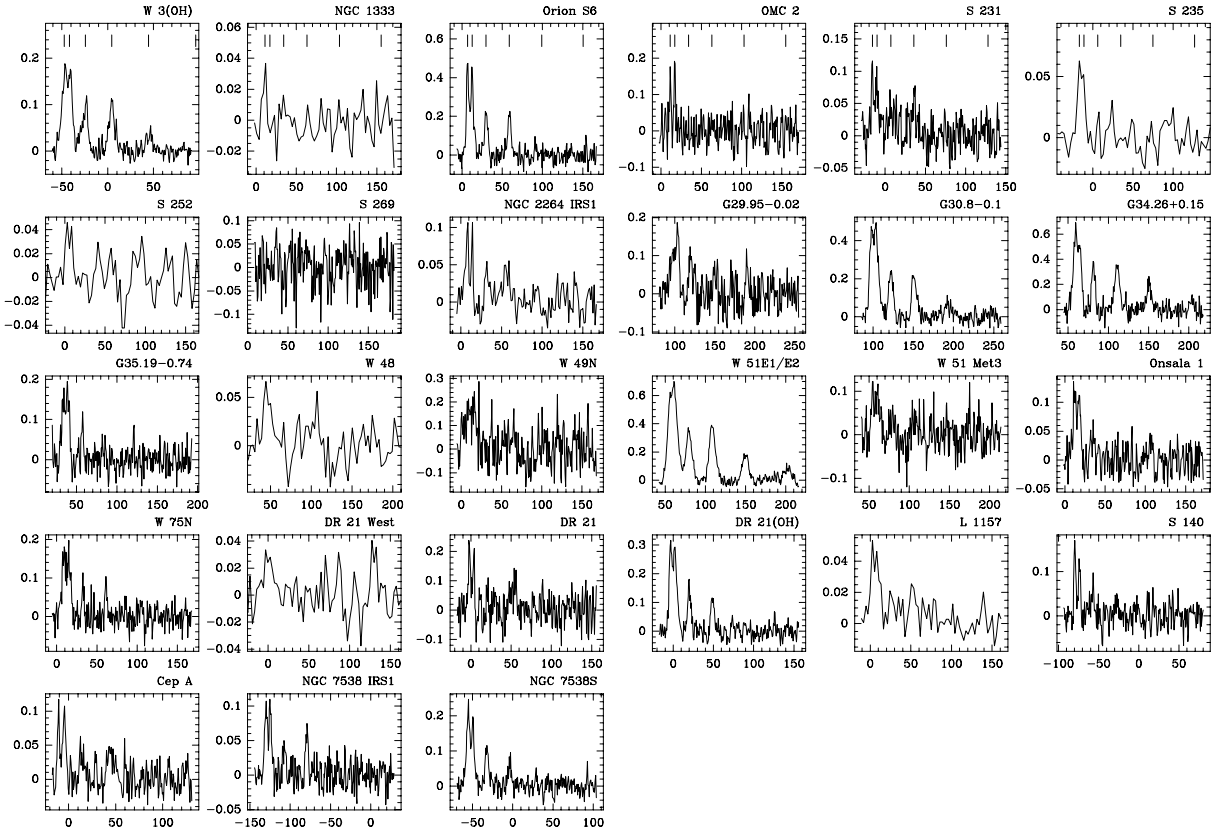

Fig. 1. Spectra of the sources, observed at 110 GHz. x-axis: LSR velocity of the $K = 0$ line in km s^{-1}; y-axis: antenna temperature in Kelvins. Vertical lines in the upper row indicate the positions of different K-components, K values increase to the right. The frequencies of the K-components are 110383.522, 110381.404, 110375.052, 110364.469 110349.659, and 110330.627 MHz for $K = 0$, 1, 2, 3, 4, and 5, respectively.

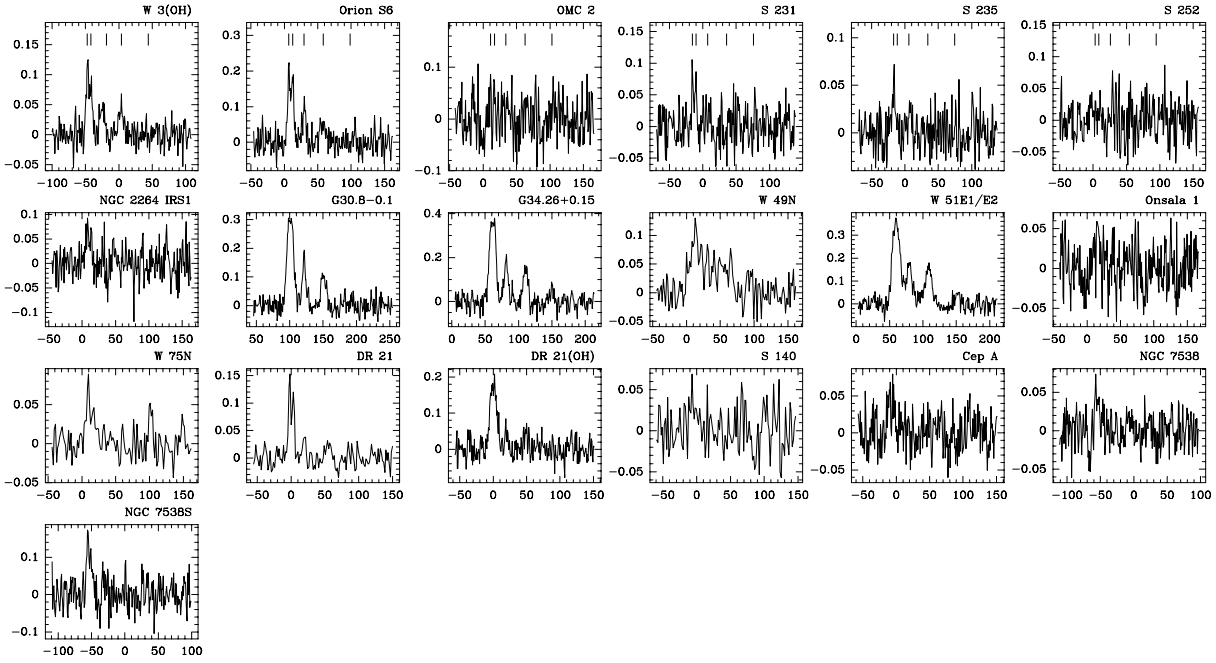

Fig. 2. Spectra of the sources, observed at 92 GHz. Axes are same as in Fig. 1. The frequencies of the K-components are 91987.090, 91985.317, 91980.089, 91971.310, and 91959.024 MHz for $K = 0$, 1, 2, 3, and 4, respectively.

Table 1. Gaussian parameters of the detected CH_3CN lines with their 1σ errors. For each source the parameters of the 110 GHz lines are given in the upper row and those of the 92 GHz lines in the lower row.

Source	R.A.$_{B1950.0}$	T_A^*dV (K km s^{-1})						V_{LSR}	ΔV
	DEC.$_{B1950.0}$	$K=0$	$K=1$	$K=2$	$K=3$	$K=4$	$K=5$	(km s^{-1})	(km s^{-1})
W 3(OH)	02 23 17.3	0.97(0.06)	1.06(0.06)	0.80(0.01)	0.79(0.04)	0.24(0.04)	<0.12	−47.5(0.2)	8.4(0.2)
	61 38 58	0.61(0.05)	0.47(0.05)	0.29(0.04)	0.27(0.04)	< 0.09		−47.5(0.2)	6.9(0.3)
NGC 1333	03 25 55.0	<0.18							
	31 04 00	not observed							
Orion S6	05 32 44.8	2.12(0.08)	2.00(0.08)	1.03(0.07)	0.83(0.07)	<0.21		6.9(0.1)	4.2(0.1)
	−05 26 00	0.97(0.07)	0.86(0.07)	0.53(0.07)	0.31(0.07)	<0.3		6.8(0.2)	4.7(0.2)
OMC 2	05 32 59.9	0.35(0.06)	0.44(0.07)	<0.18				11.2(0.1)	2.1(0.2)
	−05 11 29	< 0.11							
S 231	05 35 51.3	0.33(0.04)	0.31(0.04)	0.18(0.04)	0.23(0.04)	< 0.12		−15.9(0.2)	3.0(0.0)
	35 44 16	0.27(0.06)	0.28(0.07)	0.14(0.07)	< 0.09			−15.6(0.4)	3.8(0.5)
S 235	05 37 31.8	0.31(0.06)	0.26(0.05)	0.22(0.05)	<0.15			−17.1(0.6)	4.7(0.4)
	35 40 18	0.22(0.04)	< 0.1					−17.1(0.0)	3.7(0.0)
S 252	06 05 53.7	0.24(0.08)[1]	0.18(0.08)[1]	< 0.24				2.9(0.9)	5.0(0.0)
	21 39 09	<0.09							
S 269	06 11 46.5	<0.06							
	13 50 39.0	not observed							
NGC 2264	06 38 24.9	0.49(0.04)	0.41(0.04)	0.22(0.04)	0.17(0.04)	<0.12		8.5(0.2)	4.0(0.2)
IRS1	09 32 28	0.34(0.07)	0.26(0.07)	< 0.2				7.8(0.5)	4.0(0.0)
G29.95−0.02	18 43 27.1	0.53(0.09)	0.73(0.09)	0.51(0.10)	0.39(0.09)	0.39(0.09)	<0.27	97.6(0.2)	5.5(0.4)
	−02 42 36	not observed							
G30.8−0.1	18 45 11.0	3.09(0.11)	2.44(0.10)	1.74(0.08)	1.63(0.08)	0.58(0.07)	0.21(0.07)	98.9(0.1)	7.0(0.0)
	−01 57 57	2.18(0.16)	1.36(0.15)	1.18(0.08)	1.10(0.09)	0.32(0.08)		99.0(0.2)	7.9(0.3)
G34.26+0.15	18 50 46.1	3.72(0.15)	2.97(0.15)	2.20(0.14)	2.41(0.14)	1.31(0.13)	0.65(0.1)	58.7(0.1)	6.0(0.1)
	01 11 12	2.22(0.13)	2.06(0.12)	1.29(0.09)	1.28(0.10)	0.61(0.09)		58.5(0.2)	6.9(0.2)
G35.19−0.74	18 55 40.8	0.75(0.06)	0.88(0.07)	0.36(0.06)	<0.18			33.7(0.2)	4.6(0.2)
	01 36 30	not observed							
W 48	18 59 13.8	0.32(0.08)[1]	0.15(0.07)[1]	<0.2				43.9(0.6)	4.2(0.6)
	01 09 20.0	not observed							
W 49N	19 07 49.9	1.71(0.89)	1.69(0.98)	0.81(0.32)	1.59(0.33)	< 0.93		9.4(1.6)	16.0(1.3)
	09 01 14	1.05(0.19)	0.90(0.15)	0.99(0.15)	1.16(0.15)	< 0.45		9.2(1.0)	19.8(1.1)
W 51E1/E2	19 21 26.2	4.89(0.16)	4.21(0.15)	3.34(0.10)	3.76(0.10)	1.87(0.10)	0.67(0.07)	56.8(0.1)	9.5(0.1)
	14 24 43	2.86(0.11)	2.13(0.11)	1.63(0.11)	1.87(0.08)	0.72(0.08)		57.3(0.1)	10.8(0.2)
W 51 MET3	19 21 27.5	0.65(0.14)	0.59(0.13)	0.50(0.10)	0.42(0.11)	<0.27		55.5(0.6)	8.0(0.7)
	14 23 52	not observed							
Onsala 1	20 08 09.9	0.56(0.05)	0.55(0.05)	0.24(0.05)	<0.12			11.9(0.2)	4.7(0.2)
	31 22 42	<0.18							
W 75N	20 36 50.4	0.86(0.07)	0.84(0.07)	0.35(0.06)	0.36(0.06)	<0.18		9.4(0.2)	4.8(0.2)
	42 27 23	0.39(0.06)	0.30(0.06)	< 0.18				9.6(0.3)	4.8(0.5)
DR 21 West	20 37 07.8	0.19(0.06)[1]	0.16(0.08)[1]	< 0.21				−2.1(1.2)	5.0(0.0)
	42 08 44.0	not observed							
DR 21	20 37 13.0	0.61(0.09)	0.47(0.08)	0.16(0.08)	0.23(0.09)	< 0.21		−2.1(0.2)	2.7(0.0)
	42 08 50.0	0.63(0.05)	0.49(0.05)	0.20(0.05)	0.11(0.05)	< 0.15		−2.2(0.1)	3.7(0.2)
DR 21(OH)	20 37 13.8	1.53(0.06)	1.43(0.06)	0.74(0.05)	0.64(0.05)	<0.15		−3.1(0.1)	4.7(0.1)
	42 12 13	0.97(0.07)	1.03(0.07)	0.30(0.06)	0.25(0.06)	< 0.21		−3.0(0.2)	4.7(0.0)
L 1157	20 38 39.6	<0.09							
(0″, 0″)	67 51 33	not observed							
L 1157	20 38 41.0	0.23(0.05)	0.21(0.05)	<0.12				2.1(0.5)	4.9(0.6)
(20″,-60″)	67 50 33	not observed							
S 140	22 17 41.2	0.39(0.04)	0.30(0.04)	0.26(0.05)	<0.12			−6.8(0.1)	3.1(0.2)
	63 03 43	0.34(0.12)	0.14(0.09)	0.15(0.09)	< 0.36			−7.0(0.6)	3.8(1.1)
Cep A	22 54 19.2	0.30(0.04)	0.31(0.04)	0.08(0.03)	0.17(0.04)	<0.12		−9.9(0.2)	3.6(0.3)
	61 45 47	0.24(0.05)	0.22(0.05)	< 0.15				−10.3(0.4)	3.9(0.5)
NGC 7538	23 11 36.6	0.45(0.04)	0.42(0.04)	0.22(0.04)	0.25(0.04)	<0.12		−57.7(0.2)	4.0(0.2)
IRS1	61 11 50	0.25(0.05)	0.15(0.05)	< 0.12				−57.3(0.5)	4.0(0.0)
NGC 7538S	23 11 36.1	1.06(0.05)	0.84(0.05)	0.57(0.05)	0.34(0.04)	<0.12		−55.4(0.1)	4.5(0.1)
	61 10 30	0.74(0.09)	0.41(0.09)	0.22(0.08)	< 0.24			−55.6(0.4)	4.5(0.4)

[1] – marginal detection

Table 2. Properties of the sources obtained from SE calculations. Columns: 1, source name; 2, kinetic temperature; 3, CH_3CN abundance; 4, adopted distance; 5, angular diameter; 6, density.

Source	$T_{\rm kin}$ (K)	$X_{\rm CH_3CN}$ ($\times 10^{-10}$)	d (kpc)	θ ($''$)	$n_{\rm H_2}$ ($10^4 {\rm cm}^{-3}$)
W 3(OH)	70(50–95)	10–1000	2.2	2-4[b]	$\geq$10
Ori S6	45(40–50)	0.3–30	0.5	≥ 10	10–100
S 231	55(35–160)		2	≥ 3	
NGC 2264	45(25–65)		0.8	≥ 3	
G30.8-0.1[a]	60(45–75)	≥ 100	8	2-7	
G34.26+0.15[a]	140(65–220)	≥ 300	3.8	1-6c	
W 51E1/E2[a]	160(120–180)	100–1000	8	1-3	≥ 30
W 75N $(6'', 25'')$	40(35–60)		3	≥ 5	≥ 1
DR 21	30(20–55)		3	≥ 5	
DR 21(OH)	45(40–55)	1–100	3	≥ 8	≥ 3
NGC 7538	50(35–100)		3.5	≥ 3	
NGC 7538S	40(30–45)	10–100	3.5	5-9	10–100

[a]–core parameters
[b]–less than $1''$ according to Wink et al. (1994).
[c]–$3.9'' \times 3.3''$ (Akeson & Carlstrom 1996).

the ratios $T_{\rm mb}(6_K - 5_K)/T_{\rm mb}(6_2 - 5_2)$ and for the 92 GHz lines the ratios $T_{\rm mb}(5_K - 4_K)/T_{\rm mb}(5_2 - 4_2)$.

We modelled the CH_3CN brightness temperatures for the kinetic temperatures 10–500 K, the molecular hydrogen densities 3×10^3–10^8 cm^{-3}, and the CH_3CN densities, divided by a velocity gradient in the range 10^{-7}–10 cm^{-3}/(km s^{-1} pc^{-1}). External radiation, except the microwave background, was neglected. From these models we selected those that minimize χ^2

$$\chi^2 = \sum_i (R_{\rm i}^{\rm obs} - R_{\rm i}^{\rm mod})^2/(\sigma_{\rm i}^{\rm obs})^2 \quad (1)$$

where $\sigma_{\rm i}^{\rm obs}$ are the rms errors of the observed ratios. Then the 1σ confidence levels were calculated as described in Lampton et al. (1976).

For G30.8-0.1, G34.26+0.15 and W 51E1/E2 the minimum χ^2 values proved to be much larger than expected from the number of degrees of freedom. This is likely a result of temperature and/or density gradients in the volumes sampled by the beam (as expected in view of the limited resolution). It seems reasonable to see these sources as consisting of hot cores and colder halos. We further assumed that the core contribution dominates in the $K \geq 2$ emission and determined the "core parameters" using only the $K \geq 2$ lines. For G34.26+0.15 an interferometric hot core spectrum at 110 GHz (Akeson & Carlstrom 1996) is well approximated by our best core model, showing that this approach is reasonable.

Finally, for each model, appropriate for a given source, we estimated the source size $\theta_{\rm s}$, assuming a Gaussian brightness distribution

$$\theta_{\rm s}^2/(\theta_{\rm s}^2 + \theta_{\rm mb}^2) = T_{\rm mb}/T_{\rm mod} \quad (2)$$

where $T_{\rm mod}$ is the model brightness temperature and $\theta_{\rm mb}$ is the FWHP of the beam. For a clumpy medium the derived sizes are only lower limits since the surface filling factor of the clumps affects the observed intensity in a similar way as the size of a homogeneous source. For example, if Eq. (2) is applied to a clumpy cloud which is larger than the beam, the derived size will be smaller than the beam provided that the total surface filling factor of the clumps is less than unity.

Using published distances, we estimated source linear sizes D, averaged velocity gradients $\Delta V/D$ and CH_3CN abundance

$$X_{\rm CH_3CN} = n_{\rm m}\ \Delta V/(D\ n_{H_2}) \quad (3)$$

where $n_{\rm m}$ is the model $n_{\rm CH_3CN}/(dV/dR)$ value.

Like previous workers in the field, we found that only the kinetic temperature can be determined by this method. For most objects we could not estimate density and hence, CH_3CN abundance. To constrain these parameters, we left for further analysis only those models that agree with the ratios between the 110 and 92 GHz main-beam brightness temperatures, assuming that the latter are accurate within 20%. The results of the SE modelling are presented in Table 2.

5. Discussion and conclusions

The strongest sources in our sample are W 3(OH), G30.8−0.1, G34.26+0.15 and W 51E1/E2. With the exception of G30.8-0.1, all of them are well-known hot cores. The kinetic temperatures of these objects, except G30.8-0.1, are of the order of 100 K or higher, and the CH_3CN abundances are larger than 10^{-9}. The CH_3CN abundances of the order of 10^{-8} have been reported toward hot cores, e.g. in Orion (Blake et al. 1987) and in G10.47+0.03 (Olmi et al. 1993). The fact that the CH_3CN abundances in hot cores are increased due to evaporation of

molecular material from ice mantle of interstellar grains is well established. CH_3CN may be either a parent molecule or may be a product of a chain of gas-phase reactions, starting from HCN or some other nitrogen-bearing molecule, which appears in gas phase due to mantle evaporation (Millar 1996).

Most hot cores, observed in CH_3CN lines, are sites of massive star formation. Other regions, where gas-phase chemistry is strongly affected by grain mantle evaporation, are bow shocks at the edges of young bipolar outflows, driven by low-to-intermediate mass protostars. The temperature in these objects is high enough to evaporate grain mantles, and the contents of HCN, NH_3 and some other molecules, abundant in hot cores, are strongly enhanced. We observed two such objects, NGC 1333 IRAS2 and L 1157. In L 1157, no lines were found toward the central source ($0'', 0''$ position), but a weak emission was detected toward the blue wing of the L 1157 outflow ($20'', -60''$ position), where the abundance of HCN, NH_3, CH_3OH and some other molecules is enhanced up to several orders of magnitude (Bachiller & Pérez Gutiérrez 1997). Thus, CH_3CN may be also enhanced toward this position. Sensitive high-resolution observations are desirable to check this assumption.

The nature of the weaker sources is unclear. The data from Table 2 could suggest that Ori S6, S 231, NGC 2264, W 75N, DR 21, DR 21(OH), NGC 7538, and NGC 7538S are warm clouds with temperature of 30–50 K and methanol abundance of about 10^{-9} or lower. On the other hand, poor signal-to-noise ratios may mask their complex structure and the presence of hot gas. The nature of these sources can be established only by more sensitive observations.

Acknowledgements. We are grateful to the staff of the Onsala Space Observatory for providing help during the observations. We would like to thank Dr. V.I. Slysh for helpful discussions and Drs. C.M. Walmsley and R. Cesaroni for making available the LVG code. The work was done under partial financial support of the Russian Foundation for Basic Research (grant No 95-02-05826) and the project $N315$ "Radio Astronomy Educational and Scientific Center" within the frames of the program "State Support for the Integration of High School and Basic Research". Onsala Space Observatory is the Swedish National Facility for Radio Astronomy and is operated by Chalmers University of Technology, Göteborg, Sweden, with financial support from the Swedish Natural Science Research Council and the Swedish Board for Technical Development.

References

Akeson R.L., Carlstrom J.E., 1996, ApJ 470, 528
Bachiller R., Pérez Gutiérrez M., 1997, ApJ 487, L93
Bergman P., Hjalmarson Å., 1989, In: Winnewisser G., Armstrong J.T. (eds.) The Physics and Chemistry of Interstellar Molecular Clouds. Springer-Verlag, Berlin, p. 124
Blake G.A., Sutton E.C., Masson C.R., Phillips T.G., 1987, ApJ 315, 621
Churchwell E., Walmsley C.M., Wood D.O.S., 1992, A&A 253, 541
Lampton M., Margon B., Bowyer S., 1976, ApJ 208, 177
Millar T.J., 1996, In: van Dishoeck E.F. (ed.) Molecules in Astrophysics: Probes and Processes. Kluwer Academic Publishers, Dordrecht, p. 75
Olmi L., Cesaroni R., Walmsley C.M., 1993, A&A 276, 489
Wink, J.E., Duvert J., Guilloteau S., Güsten R., Walmsley C.M., Wilson T.L., 1994, A&A 281, 505